Deformation of Cellular Polymeric Films

Y. Rharbi,[†] F. Boué,[†] M. Joanicot,[‡] and B. Cabane*[,§]

Laboratoire Léon Brillouin, CEA-Saclay, 91191 Gif sur Yvette, France, Rhône-Poulenc, 93308 Aubervilliers, France, and Equipe mixte CEA-RP, Service de Chimie Moléculaire, CEA-Saclay, 91191 Gif sur Yvette, France

Received August 7, 1995[⊗]

ABSTRACT: Cellular films may be produced through evaporation of aqueous dispersions containing polymeric particles. The membranes of the cells are made of hydrophilic polymers which cover the particle surfaces; they form a periodic structure which separates the hydrophobic particle cores. These films are used to make adhesive coatings; in such applications, the main properties are the permeability of the film to water vapor, its mechanical resistance, and especially its resistance in wet environments. In this work, latex films have been submitted to uniaxial stretching, and the microscopic deformations of the array of membranes have been observed through small angle neutron scattering. Some films have been stretched in the dry state at a temperature above their glass transition temperature. In this case, we have found that the array of membranes was stretched uniformly according to the macroscopic deformation of the sample. Other films have been stretched in the wet state, after the membrane array was swollen with water. In this case, we have found a loss of correlation in the direction perpendicular to the stretching, indicating that the macroscopic stretching causes microscopic shear deformations.

Introduction

Polymeric films can be made through evaporation of an aqueous dispersion of latex particles.[1−4] Each particle is made of a hydrophobic polymeric core that is copolymerized with a hydrophilic membrane. Upon evaporation, the dispersion passes through three stages: (a) concentration, in which the particles are kept apart from each other by the repulsions between their membranes, and they organize into a crystalline structure to minimize these repulsions;[5] (b) contact, in which the removal of water forces each particle to come into physical contact with its 12 neighbors;[6−8] and (c) compression, in which upon removal of the remaining water, capillary forces compress the particles into dodecahedral cells. The resulting film has a foam structure where the interior of cells are hydrophobic and the cell walls are hydrophilic.[6−8]

These cellular latex films are used to manufacture coatings. In such applications, the important properties are the mechanical properties of the films and their permeability to water. The most difficult situations are those in which mechanical stress and aggression by water are combined, e.g., where mechanical resistance in a wet environment is required.

The behavior of a film under mechanical stress may be characterized by a map of the deformations. In this respect, it is important to realize that the films are composite materials, with a dispersed phase (the cell cores) surrounded by a continuous phase (the membranes). Depending on which phase is the weakest, the macroscopic deformation of the film may be achieved through deformation of all cells, or through shear deformations of the membranes, causing relative displacements of cells. The relative importance of these two types of deformations must depend on the cohesion of the membranes. For instance, in a wet environment, the hydrophilic membranes may swell with water and lose their cohesive strength.

To measure the deformations and the relative displacements of the cells, we have used small angle neutron scattering (SANS). Contrast between cell cores and membranes was obtained through addition of a deuterated solvent that was located either in the cell cores or in the membranes. The addition of a selective solvent was also used to vary systematically the strength of membranes with respect to that of cell cores. Some films were submitted to uniaxial stretching in the dry state, where the membranes were the strongest component of the material; others were stretched when the membranes were weakened by addition of water. In this paper, we present neutron scattering spectra of films stretched in these different conditions and a discussion of the modes of deformation observed in these films.

Materials

Latex Dispersions. Latex dispersions were synthesized through emulsion polymerization of styrene (S), butyl acrylate (BA), and acrylic acid (AA) in water.[6] The reaction produced polymeric particles that were 1200 Å in diameter. Each particle had a hydrophobic core made of PS and PBA sequences, surrounded by a thin layer of hydrophilic PAA and PBA sequences that were copolymerized with core polymers. A typical composition was S, 64%; BA, 32%; and AA, 4%.

In addition to the dispersed particles, the aqueous phase also contained soluble species (amphiphilic polymers, surfactant, and salt). These were eliminated through dialysis and equilibrium with ion exchange resins. After this washing process, the concentrated dispersions (5−20% latex by weight) were iridescent in visible light. This diffraction was taken as an indication of the quality of the washing process, since the ionic soluble species screen the electrostatic repulsions between particles and thus prevent their ordering.[9,10]

The surface charges of the washed latex were determined through potentiometric titration. We found 3.05×10^{-5} mol/g for sulfate groups and 2.372×10^{-4} mol/g for AA groups. The ionization of AA groups was controlled through the addition of a base (NaOH).

Film Formation. Films were made through evaporation of concentrated dispersions in an oven. The drying temperature was kept slightly above the minimal film formation temperature, T_f, which is slightly above the glass transition temperature, T_g, of the core polymer.[11] The value of T_g was set according to the proportion of S and BA ($T_g = 18$ °C for a

[†] Laboratoire Léon Brillouin, CEA-Saclay.
[‡] Rhône-Poulenc.
[§] Service de Chimie Moléculaire, CEA-Saclay.
[⊗] Abstract published in *Advance ACS Abstracts,* April 15, 1996.

S0024-9297(95)01142-9 CCC: $12.00

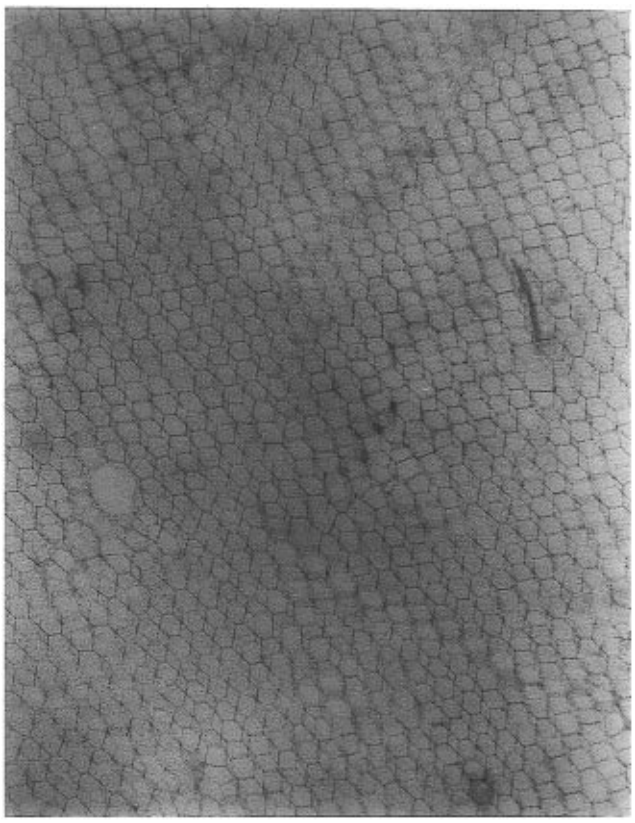

Figure 1. Electron microscopy image of a latex film sliced to 0.1 μm thickness and stained with uranyl acetate. The cells correspond to the original latex particles; the cell walls are formed by the particle membranes that have bound uranyl acetate.

48:48 ratio, and $T_g = 55$ °C at 64:32). The rate of evaporation was controlled through the relative humidity of the oven. When evaporation was slow enough, the rate of weight loss remained the same until the film was dry, indicating that the membranes remained permeable to water until they were nearly dry.

At the end of the drying stage, the properties of the membranes may change. In latex dispersions that have been neutralized with NaOH, the surface PAA polymers are polyelectrolytes, and the membranes remain hydrophilic. In latex dispersions that have not been neutalized, the surface polymers remain in the acid form, and the membranes become hydrophobic in the dry state.

An image observed through electron microscopy is shown in Figure 1.

Reswelling with Water. Most films were rehydrated to about 10% water content by weight. The reasons for rehydration were twofold. First, the addition of a deuterated solvent (D_2O) gave contrast in neutron scattering. Second, the properties of the swollen films were also of interest.

We found that all films made with unwashed latex could be rehydrated easily, because the soluble species that were initially in the aqueous phase had become trapped in the membranes. Films made from washed latex could also be rehydrated easily if the latex dispersion had been neutralized with NaOH. In this case, the maximum water content after reswelling was 50%. Films made from latex that had been washed and kept in the acid form took up very little water (on the order of 2%), for reasons explained above (Figure 2).

Small Angle Neutron Scattering

Technique. Concentrated latex dispersions and the films made from them have long range order.[5−8] Therefore, they can diffract radiations of appropriate wavelength. The directions of diffraction and the relative intensities in these directions are related to repetitions

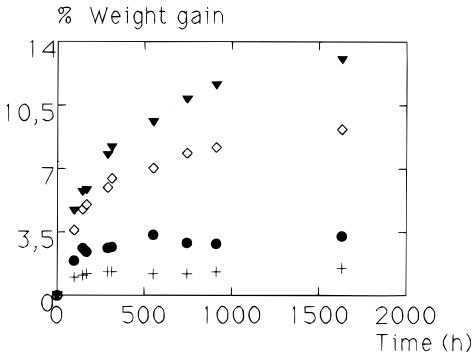

Figure 2. Rehydration of "hard" films ($T_g = 55$ °C) at 35 °C. Vertical axis: weight gain as a percentage of the film weight. Horizontal axis: time in hours. The data show that the water uptake depends strongly on pH. ●, Films from latex kept in the acid form at pH 2. ◇, Films from latex partly neutralized at pH 7 by NaOH. ▼, Films from latex fully neutralized at pH 10 by NaOH. +, Films from latex neutralized by $Ba(OH)_2$ at pH 7.

of the unit cell in the lattice and to the structure of this unit cell. For crystalline systems that have periods of 0.1 μm, small angle neutron scattering is appropriate.

The measurements were made on the instrument PAXY of LLB. The wavelength of incident neutrons was chosen between 3.5 and 15 Å, and the sample-to-detector distance was set between 2 and 7 m. The scattered neutrons were collected on an XY (64 × 64) multidetector. The map of collected intensities yields a two-dimensional image of the reciprocal lattice of the sample along a plane normal to the beam. Later, the collected intensities may be regrouped, either according to angular sectors of the detector, if the scattering is anisotropic, or according to circular rings, if it is isotropic. This regrouping yields spectra of the intensity I according to the magnitude q of the scattering vector. The range of accessible q values is 2×10^{-3} Å$^{-1} < q < 2.5 \times 10^{-2}$ Å^{-1}, corresponding to a range of real-space distances 240 Å $< 2\pi/q <$ 3000 Å.

Diffraction Patterns. When the latex particles are all of the same size, their packing in a film gives a periodic structure with face-centered cubic symmetry (fcc).[5−8] Depending on the method of fabrication of the film, this structure may grow in many small crystallites that have random orientations or in a large single crystal. In the former case, the diffraction pattern is made of rings (Figure 3); in the latter case, the diffraction pattern is made of spots corresponding to the points of the reciprocal lattice that are in the diffraction condition (Figure 4).

The highest intensities in the diffraction pattern usually originate from diffraction by the densest planes of the structure.[12] In Figure 3, the radius of the ring is at $q = 6.8 \times 10^{-3}$ Å^{-1}; this corresponds to the distance between (111) planes of particles, which are the densest planes of the fcc structure. This is confirmed by the 6-fold symmetry of the single crystal pattern of Figure 4, which matches the symmetry of the fcc structure in a (111) plane. In a perfect fcc structure, there would be an extinction of the (111) spots; since these spots are observed here, we conclude that faults in the repetition of planes remove this extinction. The next set of six spots in this pattern is made of [220] reflections, which are exactly in the Bragg condition since the (220) planes are normal to the beam.

Contrasts. Small angle scattering is produced because the structures are made of the repetition of regions that have different contrast for the radiation.

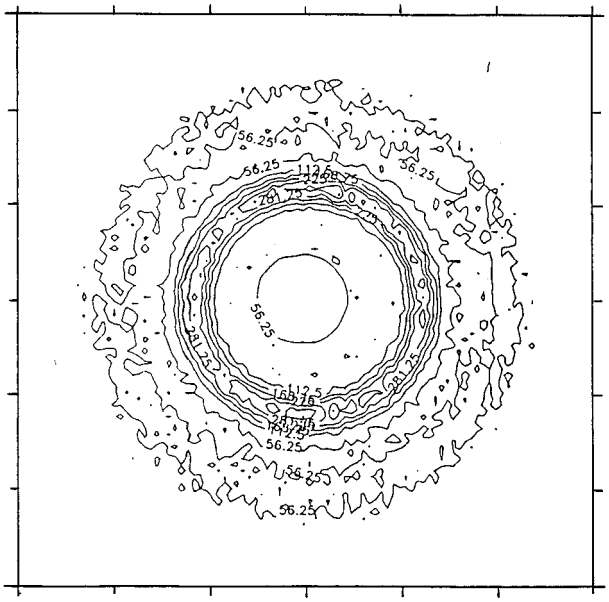

Figure 3. Diffraction pattern from a polycrystalline latex film. The figure is a contour map of the intensity levels obtained on the two-dimensional detector.

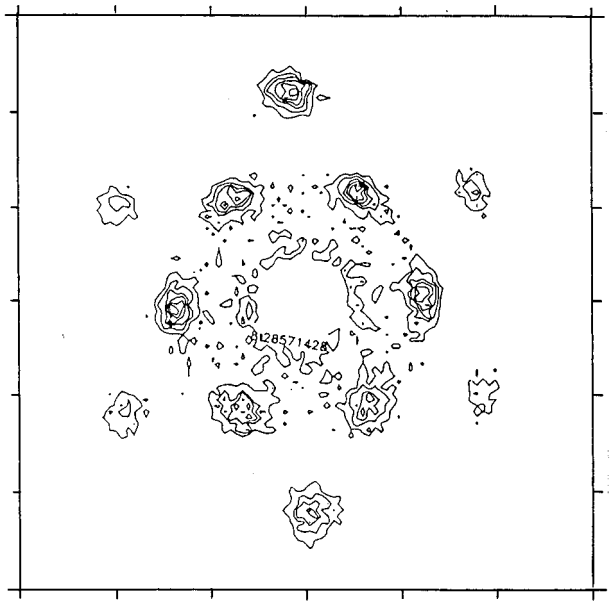

Figure 4. Diffraction pattern from a single-crystal latex film. The six diffraction spots closest to the beam correspond to the 111 reflections of the fcc structure; they give the first diffraction ring observed in polycrystalline samples. The next step of spots corresponds to the 220 reflections.

In the case of latex films, it is desired to have contrast between cell cores and cell membranes and also contrast for defects in the structure. Neutrons are scattered by nuclei in the sample; good contrast is obtained by replacing H nuclei with D nuclei. A simple way of introducing D nuclei is to swell the films with deuterated solvents, e.g., D_2O, which is preferentially adsorbed by hydrophilic PAA polymers, benzene, which is preferentially absorbed by PS, and methanol, which is absorbed by PBA and PAA. In the following, we shall analyze the way in which these solvents are distributed in the film structures. This analysis is particularly important for films that are stretched in the swollen state, since this distribution may affect the relative strengths of different regions of the films.

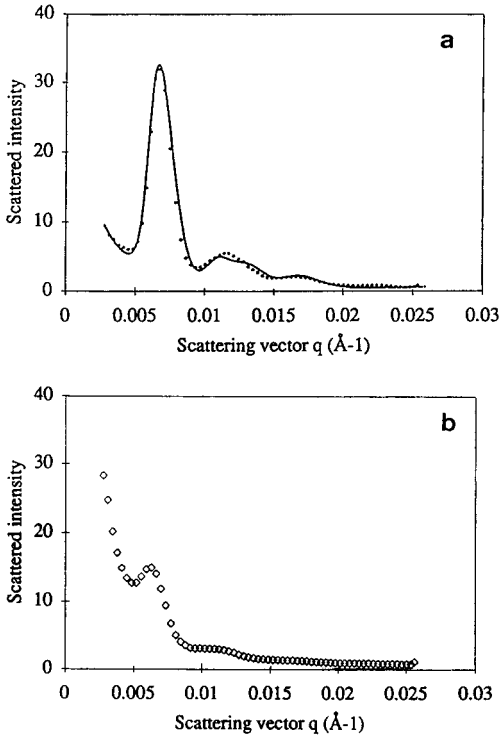

Figure 5. Comparison of diffraction spectra from different films. These spectra have been obtained through isotropic regrouping of intensities collected in two-dimensional patterns. (a) Latex washed with NaOH at pH 10 and rehydrated with D_2O. (b) Latex washed at pH 2. The comparison shows that the localization of water in the stucture has changed. The fit indicated in (a) corresponds to the scattering calculated for a fcc packing of dodecahedra with D_2O in the membranes.

Localization of Deuterated Solvents in the Films. In geometrical terms, there are three possible locations for these deuterated solvents: the cell cores, the membranes, and large defects in the structure. The localization of a particular solvent depends on the chemical nature of these three regions. For instance, the membrane polymers (PAA) are hydrophilic when they are neutralized but hydrophobic when they are in the acid form. Therefore, there is a possibility that, in films made of latex in the acid form, water does not localize preferentially in the membranes. This problem was examined by comparing the scattering and the amount of water uptake from both types of films.

Figure 5a shows an isotropic regrouping of the intensity scattered by a film made from neutralized latex and rehydrated with D_2O. The high intensity of the diffraction peak and the absence of scattering outside the peak demonstrate that the water is localized on a periodic lattice. This lattice must be the array of membranes, since the neutralized PAA polymers are the most hydrophilic component of the film. Moreover, there is no other location in the film where it would be possible to localize so much water (up to 50% of the film weight). Figure 5b shows the corresponding spectrum for a film made from latex in the acid form and also equilibrated with D_2O. The low intensity of the peak and the high intensity next to the beam demonstrate that the distribution of water is different. Two interpretations may be given at this stage: either the films made from latex in the acid form have the same ordered structure as the films made from neutralized latex, but the localization of water is different, or these films have lost the ordered structure. This loss of the ordered structure could result from fragmentation of the particle

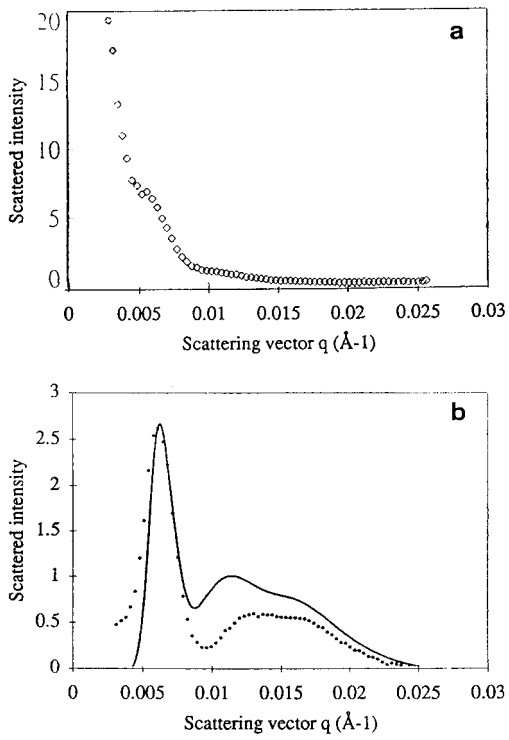

Figure 6. Comparison of diffraction spectra from two samples of the same film made of acid latex. NaCl was added to improve the penetration of solvents in the film. In (a) the film was rehydrated with D_2O and in (b) with CD_3OD (20%). The strong first diffraction peak observed with CD_3OD demonstrates that the films have a periodic structure, and the strong scattering at $q \rightarrow 0$ observed with D_2O shows that water is localized in the defects of the film. The fit indicated in (b) corresponds to the calculated scattering from a cellular fcc structure with CD_3OD in the outer PBA regions of the cells and in the PAA membranes.

membranes and fusion of the particle cores. However, previous studies have demonstrated that, in films with this composition, such fragmentation occurs at temperatures higher than the film formation temperature (70 °C) and only after long annealing times (24 h). Therefore, the second interpretation may be considered unlikely.

This ambiguity may be resolved by swelling the same films with CD_3OD instead of D_2O. Figure 6a shows the spectrum from a film prepared from latex in the acid form with salt and later rehydrated with D_2O; this shows, as above, a weak diffraction peak and a strong scattering next to the beam. Figure 6b shows the spectrum from the same film swelled with CD_3OD; this shows a strong diffraction peak and no scattering next to the beam. Since the film is the same, it may be concluded that all these films have an ordered structure, but the localization of water has changed according to the polarity of the membranes. Accordingly, in films made of latex in the acid form, D_2O was excluded by the PAA membranes and localized in the defects that contained the added salt, whereas CD_3OD was still taken by the ordered structure.

From these experiments, we conclude that films made of neutralized latex take up D_2O in their membranes in large amounts (up to 50% of the film weight), whereas films made of latex in the acid form take up D_2O only in their defects in small amounts (2% of the film weight).

Localization of Deuterated Solvents in the Unit Cell. The precise location of solvents in the unit cell of the structure can be resolved through an analysis of peak positions and intensities. For films made of neutralized latex and rehydrated with D_2O, the spectra consisted of an intense first peak and a weaker second peak (Figure 5a); the ratio q_2/q_1 varies between 1.78 and 1.83, according to swelling. These positions do not match the ratio expected for the [111] and [220] peaks of the fcc structure, which is $q_2/q_1 = 1.63$. For films reswelled with methanol (Figure 6b), both peaks are intense, and the second one is broad; the ratio of their q values is $q_2/q_1 = 2$. This ratio is also larger than that expected for the [111] and [220] spots. These shifts and broadenings indicate that the observed peaks contain more diffraction lines than just [111] and [220].

To analyze precisely the contributions of various diffraction lines, we have calculated the difraction spectrum according to the following expression:[12]

$$I(q) = \sum_i f_i (q q_i)^{-1} P_i(q_i) S_i(q, q_i, \sigma_i) \qquad (1)$$

where $\sum_i$ is a summation over successive diffraction lines located at $q = q_i$, f_i is the number of diffraction spots (multiplicity) that contribute to each line, $(qq_i)^{-1}$ is the Lorentz factor that counts the number of crystallites that are in the Bragg condition at q_i, $P_i(q_i)$ is the form factor that describes the interferences within the unit cell in this direction, and $S_i(q,q_i,\sigma_i)$ is a Gaussian function of width σ_i and unit area that describes the shape of each line. The form factor must be calculated for a dodecahedral cell of parameter a, where the deuterated solvent penetrates an outer shell of thickness b; the expressions are given in Appendix A.

The resulting fit to the spectrum of the film swollen with D_2O is shown in Figure 5a; the fit parameters are given in Appendix A. The first peak is a combination of the [111] and [200] lines; its position is quite close to that of the [111] line. The second peak turns out to be a combination of the [220], [311], [222], and [400] lines; its position is shifted to high q compared with the [220] line. This explains the anomalous values of q_2/q_1. The regular oscillation of the intensity is reproduced by a dodecahedral cell with $b/a = 0.13$; this value is consistent with the confinement of D_2O in the thin-cell membranes.

The fit for the film swollen with CD_3OD is shown in Figure 6b. The second peak is a broad hump that contains intensity from the [220], [311], [222], [400], [331], [420], and [422] lines. The fit was obtained with $b/a = 0.8$; this value indicates that methanol swells the membrane and a large part of the cell core; only the pure PS part of the core is not solvated.

These estimates of solvation by water and by methanol are in agreement with the glass transition temperatures of the films. For the film rehydrated with water, T_g is nearly the same as that of the dry film, whereas for the film swollen with methanol, it is considerably lower. A picture of the structures indicating the extent of solvation by water and by methanol is presented in Figure 7.

Mechanical Properties of Latex Films

In this section we describe the macroscopic deformations that occur in films when they are submitted to mechanical stress. Since the films are composite materials made of cell cores separated by membranes, their behavior under mechanical stress depends on the relative strengths of these two components. Accordingly, we first give a mechanical description of each component, then we examine how they contribute to the

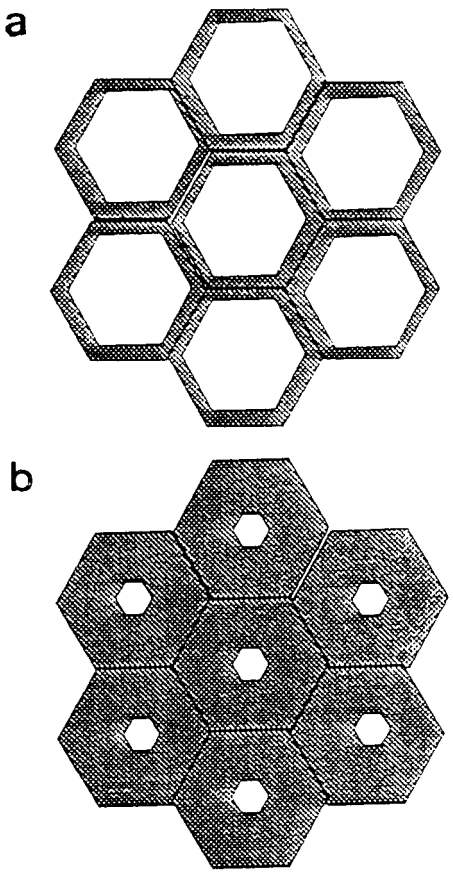

Figure 7. Localization of solvents in the cellular film structures. (a) Swelling by D_2O; the region where water is localized has been determined according to the fit of the diffraction spectrum in Figure 5a. (b) Swelling by CD_3OD; the region where methanol is localized has been determined according to the fit of the diffraction spectrum in Figure 6b.

mechanical resistance of the films. The resistance of the films was measured in a stretching experiment, where a sample of dimensions 1 mm × 10 mm × 50 mm was elongated at increasing stretching ratios λ, and we recorded the force applied at each value of λ, as well as the value λ_r where the film ruptured.

Mechanical Description of the Cell Cores. The cell cores are made of a melt of BA copolymers with a high molar mass, $M_w > 5 \times 10^5$. This melt has a very broad distribution of relaxation times; the longest time, t_{ter}, corresponds to the rate of disentanglement processes.[13] All these times are determined by the value of the temperature with respect to the glass transition temperature of the copolymers: the longest time t_{ter} remains very long when the temperature is kept below T_g + 25 °C and becomes as short as 1 s when the temperature reaches T_g + 75 °C. Thus, the material becomes fluid either at elevated temperatures or upon addition of a solvent that localizes in the cores and lowers the T_g.

Mechanical Description of the Membranes. The membranes are made of copolymers that contain a large proportion of PAA; in the dry state these polymers are held together by hydrogen bonds between their acid groups or by clusters of ion pairs originating from the neutralization of these groups. In the bulk, these polymers have a high glass transition temperature (T_g = 140 °C). However, the membranes are quite thin (10−20 Å) and also contain some BA monomers; therefore, the bulk glass transition temperature is not a good indication of the temperature range where the membranes are strong. A better indication is provided by the temperature at which the membranes are fragmented and the cell cores fuse together.[14] This temperature depends on the mobility of the core polymers and on the presence of cations in the membranes. For the latex films in the acid form, this temperature is 100 °C; for latex films in the neutralized form, it is 180 °C.

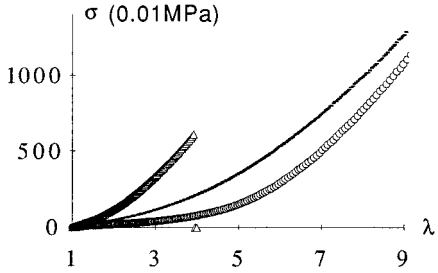

Figure 8. Apparent modulus of dry films stretched at a temperature T_g + 25 °C and at a slow rate $S = (1/L)(dL/dt) = 0.0016\ s^{-1}$. Vertical axis: modulus, in 10^{-2} MPa. Horizontal axis: deformation $\lambda = L/L_o$. Dashes: film made from latex washed at pH 2; the array of membranes is fully connected. Dots: film made from the same latex and annealed for 24 h at 120 °C; the array of membranes has been fragmented. Triangles: film made from latex washed at pH 10; the array of membranes is reinforced by Na cations.

Effect of the Connectivity of the Membranes. Even though the membranes are quite thin, their contribution to the mechanical strength of the films is important, as long as they retain their connectivity. This is demonstrated by a comparison of films that have a fully connected network of membranes with films that have been annealed at a temperature where the membranes are fragmented. The latex was in the acid form, with a core glass transition temperature T_g = 55 °C. Experiments were performed at 80 °C; at this temperature, the longest time t_{ter} is still quite long, and the measured instantaneous modulus may be assimilated to an elastic modulus. The results are presented in Figure 8; they show that the film with fragmented membranes has a lower modulus than the film with a fully connected membrane array.

In the following, we shall consider only films that have fully connected membrane arrays. These films are composite materials made of a dispersed phase, the cell cores, in a continuous phase, the network of membranes.

Effect of the Strength of the Membranes. (i) Strong Membranes. In dry films made of latex in the acid form, the contributions of membranes and cell cores to the modulus of the films are comparable, as demonstrated in Figure 8. Situations where the membranes are stronger than the cores may be obtained in two ways. The membranes may be reinforced by cations if the films are made of neutralized latex and if they are kept in the dry state. This effect is also demonstrated in Figure 8: the film made of neutralized latex has a much higher modulus and breaks at a lower deformation (λ = 4.5) than the film made of latex in the acid form (λ > 8). An even stronger reinforcement may be obtained using divalent cations.[4] Alternatively, the cores may be weakened by swelling with a selective solvent, e.g., benzene or toluene. In this case, the modulus is lower than that of the unswollen film, but the film breaks at the same value of the deformation, indicating that its mechanical failure is controlled by the state of the membranes (Figure 9b).

Comparing all these situations, we find that the modulus is controlled by the cores and membranes (compare films with and without benzene) but that the

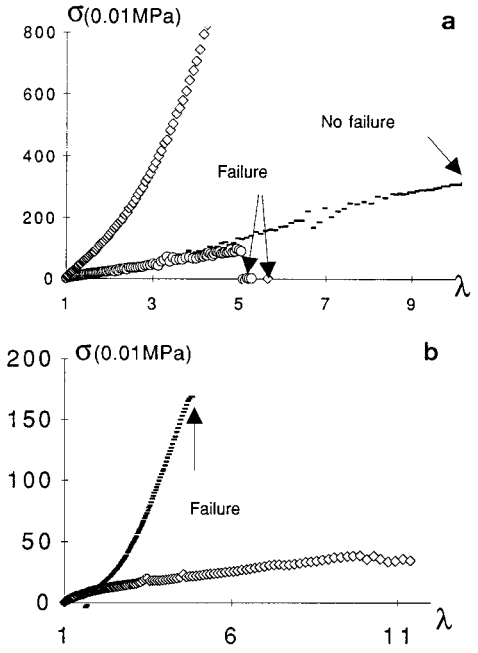

Figure 9. (a) Apparent modulus for dry and for wet films stretched as in Figure 8. Diamonds: dry film made from latex neutralized at pH 10; this film is quite strong and breaks at low stretching, as indicated on the horizontal axis. Dashes: film swollen at 15% with water; this film is easy to stretch and breaks only at large stretching, beyond $\lambda = 11$. Circles: film swollen at 35%; this film is easy to stretch and breaks at low stretching, as indicated on the horizontal axis. (b) Apparent modulus for films reswelled with organic solvents. Dashes: films made of latex washed at pH 2 with added salt, swollen with benzene (23% of the film weight). Diamonds: same with methanol instead. The stretching curve of the benzene-swollen film results from elastic resistance of the membranes (compare with Figure 8). The stretching curve of the methanol-swollen film corresponds to viscous flow of the film under the applied force.

mechanical failure occurs at a maximal strain that is determined the membranes only (compare films with acid and with neutralized membranes).

(ii) Weak Membranes. The membranes may be weakened by the introduction of a selective solvent: water, for films made of neutralized latex, or methanol, for all films containing AA and BA monomers in their membranes.

Films made of neutralized latex were rehydrated through exposure to water vapor at various water contents and then stretched at $T_g + 25$ °C, still in presence of water vapor; the results are presented in Figure 9a. At low water contents (<5%), the modulus remains high and the films break at a rather low deformation ($\lambda_r < 5$); up to that point, the deformation is recoverable upon releasing the applied force, as it is in dry films. At intermediate water contents (10−15%), the modulus drops, and the maximum deformation reached before breaking increases considerably ($\lambda_r > 17$). Only the moderate deformations ($\lambda < 3$) are recoverable upon releasing applied force; larger deformations are not recoverable, indicating that viscous flow (creep) took place in the sample. Finally, for the highest water contents (35%), the modulus is very low, and the films break at low values of the deformation ($\lambda_r < 5$).

Films made of latex in the acid form, with added salt, were swollen through exposure to methanol in a closed container, and then stretched at $T_g + 25$ °C, still in presence of methanol vapor. It is instructive to compare these results with those obtained on the same latex swelled with benzene; the comparison is presented in Figure 9b. On the one hand, the stretching curve of the film swelled with benzene resembles that of the dry film, obtained at a higher absolute temperature; moreover, the deformation is fully recoverable up to the point where the film breaks, which is reached at a low value of the deformation ($\lambda_r < 5$). These features indicate that the stretching curve is controlled by elastic resistance of the membranes. On the other hand, in the stretching curve of the film swollen with methanol, the initial elastic resistance (recoverable) is followed by a long stage of easy creep (not recoverable). This behavior indicates that the applied force causes viscous flow in the continuous phase of the dispersion, i.e., in the membranes.

Structures of Deformed Films

In this section we describe the microscopic deformations that occur in films when they are submitted to mechanical stress. Since the films are composite materials made of cell cores separated by membranes, their microscopic deformations may depend on the relative strengths of these two components. For this purpose, films were examined through neutron scattering after they had been stretched in conditions where the membranes were either the strongest or the weakest component of the composite.

Structures of Films with Strong Membranes. This situation is encountered in three cases: (i) dry films with membranes in the acid state, where the membranes and cores are of comparable strength; (ii) dry films with membranes reinforced by cations, in which case the membranes are strongest; and (iii) films swollen with an apolar solvent, which weakens the cores in comparison with the membranes. In these conditions, the mechanical response of the films to a macroscopic deformation is mainly elastic (see above).

(i) Dry Films, Acid Membranes. These films were stretched in the dry state, at high temperature ($T = T_g + 25$ °C), in a bath of siloxane oil. In these conditions, the modulus of the films is low, and they can be stretched to large deformations, up to $\lambda = 10$. The films were then cooled in air while the deformation was maintained. After cooling, the stress could be released without losing the deformation, since room temperature was below T_g. Finally, the films were rehydrated with D_2O for the observation through neutron scattering.

For films that take up water readily, there was a concern that the structure of the sample might be affected by the rehydration. We checked this through neutron scattering and found that the microscopic structure remains unchanged as long as the uptake of water does not exceed 10% of the film weight. However, the macroscopic shape of the samples was found to become distorted when the rehydration ratio exceeded 10%. Thus, high rehydration ratios were avoided. For films that do not take up water readily, it was difficult to obtain a uniform distribution of water throughout the membranes rather than in the defects of the film. This difficulty arose in samples made of washed latex in the acid form, where the membranes are quite hydrophobic. Instead, we used films made of unwashed latex, where the membranes contain small hydrophilic species that can be rehydrated.

At low values of the deformation, up to $\lambda = 2.5$, the diffraction ring becomes an ellipse with the short axis in the stretching direction. The intensity is weakest in this direction and strongest in the perpendicular direc-

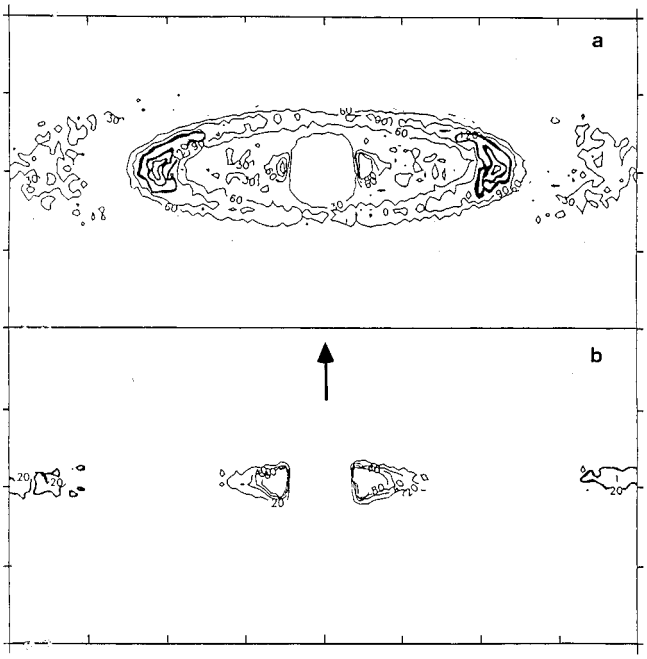

Figure 10. Diffraction patterns from polycrystalline films stretched in the dry state at $T_g + 25$ °C and then quenched at room temperature and rehydrated with D_2O. (a) Final deformation $\lambda = 2.4$. The diffraction was obtained with the stretching direction along the arrow. The deformation of the originally circular ring into an ellipse and the reinforcement of this ellipse in the direction perpendicular to the stretching are characteristic of an affine deformation. (b) Final deformation $\lambda = 7$. The two diffraction spots near the edges of the detector are all that remain from the diffraction ellipse. These spots indicate that the stretched membranes form a lamellar structure oriented along the stretching direction. The scattering near the beam in the horizontal direction correspond to defects that are elongated in the stretching direction.

tion (Figure 10). The dimensions of the ellipse correspond to the inverse diameters of the unit cell of the structure; they vary according to the macroscopic deformations. In the stretching direction, the sample is elongated in a ratio λ, and the diameter of the ellipse is compressed as λ^{-1}. In the perpendicular direction, both transverse dimensions of the sample vary as $\lambda^{-1/2}$ because the sample volume is conserved, and the diffraction ellipse is stretched as $\lambda^{1/2}$. Moreover, the distribution of intensity along the ellipse also matches the scattering expected from an affine deformation of the sample. The detailed analysis is presented in Appendix B; it shows that the distribution of intensity on the ellipse can be reproduced if it is assumed that each crystallite is deformed and reoriented by an affine deformation field. These observations demonstrate that each cell is deformed in the same way as the whole sample, indicating that the deformation field is affine.

At higher deformations, the ellipse continues to stretch and strengthen in the direction perpendicular to the stretching, while it weakens and becomes nearly invisible in the stretching direction (Figure 10). In the end, the scattering is concentrated in two diffraction spots located at the extremities of the ellipse. This pattern indicates that most membranes have been stretched so much that they are nearly parallel to the stretching direction; the two spots correspond to diffraction by this lamellar structure. The distance between the spots measures the thickness of the cells in the perpendicular direction; it is still affine to the macroscopic deformation, at least up to $\lambda = 7$ (Figure 11).

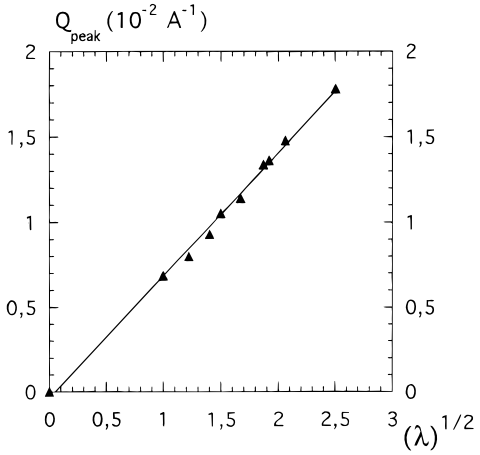

Figure 11. Deformation of the unit cell according to the diffraction patterns. Horizontal axis: square root of the macroscopic deformation λ. Vertical axis: relative variations of the large axis of the diffraction ellipse. This yields the microscopic compression of the unit cell in the direction perpendicular to the stretching. The relation of proportionality indicates that the microscopic deformations are affine to the macroscopic deformation.

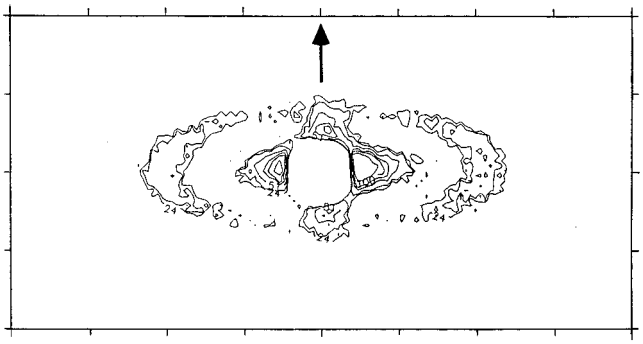

Figure 12. Diffraction from a film that was stretched in the dry state up to $\lambda = 2$, annealed at $\lambda = 2$, and then quenched at room temperature and rehydrated with D_2O. The scattering next to the beam in the horizontal direction corresponds to preexisting defects that were stretched along the stretching direction. The scattering next to the beam in the vertical direction corresponds to cracks that propagate perpendicular to the stretching direction.

In addition to this diffraction by the periodic lattice of membranes, the patterns also show diffuse scattering caused by defects. In films that have been quenched immediately after stretching, diffuse scattering is localized mainly next to the beam in a set of "whiskers" that are elongated in the direction perpendicular to the stretching. This scattering corresponds to defects that are elongated in the stretching direction; they may be air bubles or water pools that preexisted the stretching and were stretched so much that their thickness caused scattering in the range of accessible q vectors. Since the films are still far from their breaking point, it may be concluded that such defects do not alter their mechanical resistance. However, when the films are annealed at the stretching temperature in the stretched state, they show additional diffuse scattering next to the beam but in the stretching direction (Figure 12). This scattering corresponds to cracks that are elongated in the direction normal to the stretching. Such cracks, which propagate normal to the stretching, could cause the stretched films to break.

(ii) Dry Films, Neutralized Membranes. These films were obtained from latex dispersions that had been neutralized to pH 10 with NaOH; when they are

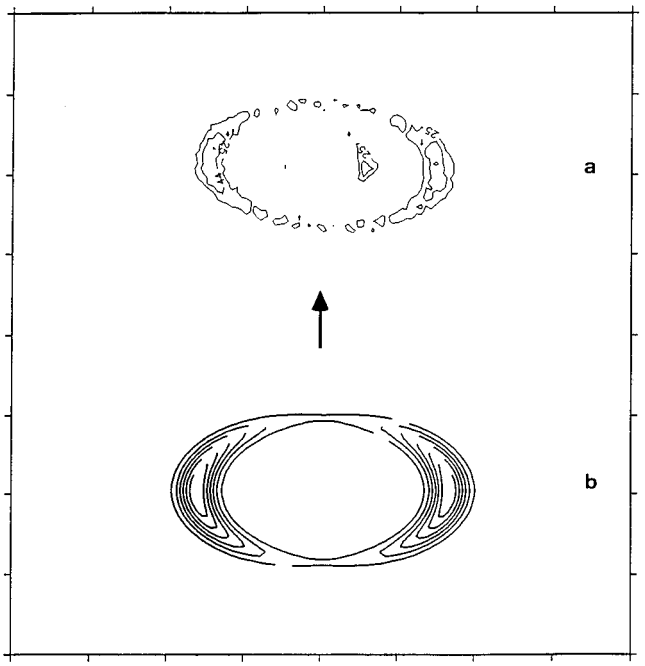

Figure 13. (a) Diffraction from a film that was swollen with benzene (23% of the film weight) and stretched in the swollen state up to $\lambda = 1.5$. The pattern is typical of an affine deformation, obtained when the membranes are stronger than the cell cores. (b) Calculated scattering pattern for an affine deformation of a polycrystalline sample (see Appendix B for details). The arrow indicates the direction of stretching.

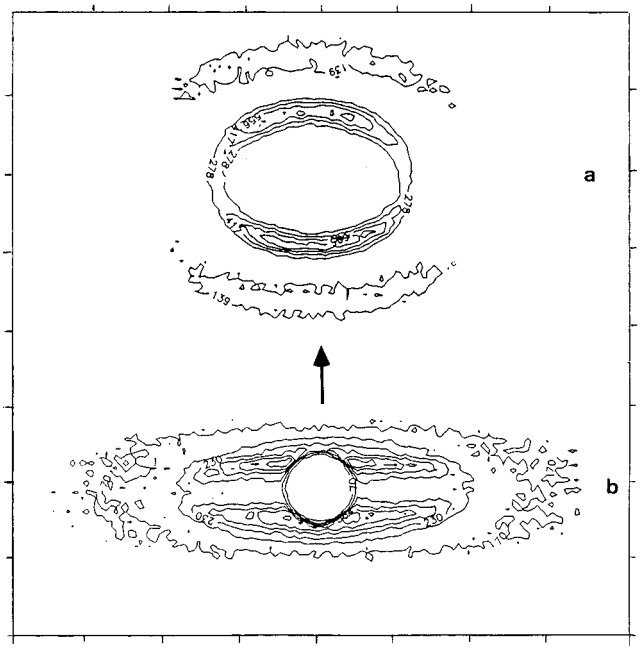

Figure 14. (a) Diffraction from a film stretched at high water content (19% D_2O) and high temperature ($T_g + 25$ °C) up to $\lambda = 1.25$. The distribution of intensity on the first-order diffraction ring is opposite to that observed with films stretched in the dry state (compare with Figure 10). The same distribution of intensity is observed on the second-order ring. (b) Diffraction from the same film stretched to $\lambda = 3$. The first-order diffraction ring is transformed into a set of two stripes spaced along the stretching direction and elongated in the perpendicular direction. The second diffraction order has merged with the first.

dry, their membranes are reinforced by association of (COO^-/Na^+) ion pairs.[14] As explained in the Mechanical Properties section, these films have a high modulus, but they break at a low stretching, in the vicinity of $\lambda_r = 5$. The diffraction patterns of these films are generally similar to those presented in Figures 10 and 12. However, near the breaking point, a nearly isotropic scattering appears next to the beam. Since the film is on the verge of breaking, it may be reasonable to assume that this isotropic scattering is caused by regions of the sample where the stress has been released by the propagation of cracks.

(iii) Films Swollen by an Apolar Solvent. Similar films were swollen with deuterated benzene or toluene (23% of the film weight), stretched in the swollen state, and observed through neutron diffraction. All operations took place in a closed container that was saturated with benzene or toluene vapor. In these conditions as well, the membranes are the only strong component of the composite. The diffraction pattern is shown in Figure 13a; it is similar to that presented in Figure 10a. Comparison with the calculated spectrum (Appendix B and Figure 13b) shows that the distribution of intensity along the diffraction ellipse is that expected for an affine deformation of a dodecahedral cell.

Structures of Films with Weak Membranes. This situation was encountered in two cases: (i) films with neutralized membranes, swollen with water and stretched in the swollen state, and (ii) films with acid membranes, swollen with methanol and stretched in the swollen state. In these conditions, strong uniaxial stretching causes plastic deformation of the films (see Mechanical Properties of Latex Films).

(i) Films with Neutralized Membranes, Swollen with Water. These films were obtained from latex dispersions that had been neutralized to pH 10 with NaOH. They were placed in a closed container saturated with D_2O vapor at a temperature $T = T_g + 25$ °C. When the swelling was sufficient, they were stretched in a few minutes, and then the container was cooled down while the deformation was maintained. Finally, the films were examined through neutron scattering.

For polycrystalline samples, the first diffraction ring is again deformed into an ellipse with the long axis along the direction normal to the stretching. However, the distribution of intensity on this ellipse is opposite to that observed in dry films: in the present case, the intensity is weak in the perpendicular direction and strong in all other directions (Figure 14a). With increasing deformations, the first-order ring is progressively transformed into a set of two stripes that are centered on the stretching direction and elongated in the perpendicular direction. The second-order ring deforms in the same way and merges with the first ring when the stretching is very high (Figure 14b).

These patterns may be analyzed to give a picture of the objects that cause the scattering. In the direction of stretching, the diffraction pattern is periodic; accordingly, the objects that cause the scattering must be repeated in this direction. Since the stripes are located on the ellipse resulting from deformation of the original diffraction ring, the repetition of these objects matches the repetition of the deformed cells. In the other directions of the pattern, there are no repetitions; therefore, the objects are not correlated in any other direction. Moreover, the stripes are narrow in the stretching direction and elongated in the perpendicular direction; accordingly, these objects must be quite elongated in the stretching direction and thin in the perpendicular direction. Consequently the objects that produce the stripes may be described as "strings" that are oriented along the stretching; each string is made

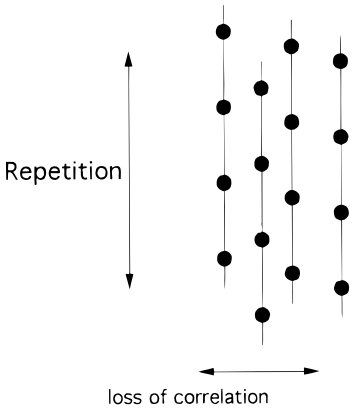

Figure 15. Picture of the defects that cause the scattering in stripes shown in Figure 14. Each "string" is made of thin water pools that are repeated along the stretching direction; neighboring strings are not correlated in any direction.

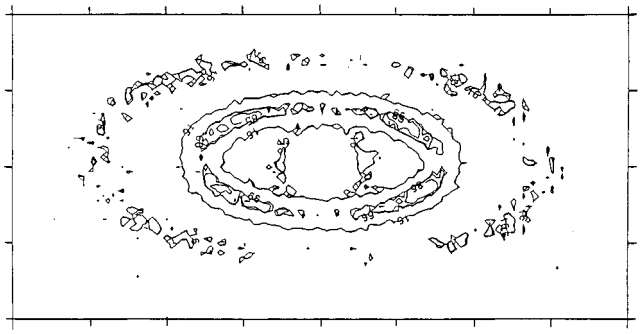

Figure 16. Diffraction from a film stretched at intermediate water content (12% D_2O) up to $\lambda = 1.71$. This diffraction pattern represents a type of deformation that is intermediate between the elastic deformation shown in Figure 10 and the plastic deformation shown in Figure 14.

of thin water pockets that are repeated at each cell, and neighboring strings are not correlated in any direction (Figure 15).

This transformation of the scattering pattern is characteristic of films where the membranes are weakened by water, and the mechanical behavior has changed from elastic to plastic (see the Mechanical Properties section). Observation of films that were stretched at different water contents showed that the change was progressive with the increase in water content. At low water contents (<5%), where mechanical testing shows elastic deformation, the diffraction pattern was an ellipse reinforced in the perpendicular direction, as in the films with strong membranes. At intermediate water contents, between 5% and 15%, the intensity shifted to four spots located out of the perpendicular direction (Figure 16). This pattern indicates that the correlations had shifted from the perpendicular direction to an oblique direction. At still higher water contents, between 15% and 25%, the four spots merged to form the stripes shown in Figure 14b, indicating that correlations were retained only in the stretching direction. At the highest water contents, beyond 25%, the stripes become broader and shorter, indicating that even in the stretching direction, the repetitions become irregular.

Another way of changing the relative strengths of membranes and cell cores is to change the stretching temperature; indeed, the strength of the cell cores varies rapidly near their glass transition temperature T_g, while the rehydated membranes remain weak regardless of the temperature. The experiments described above

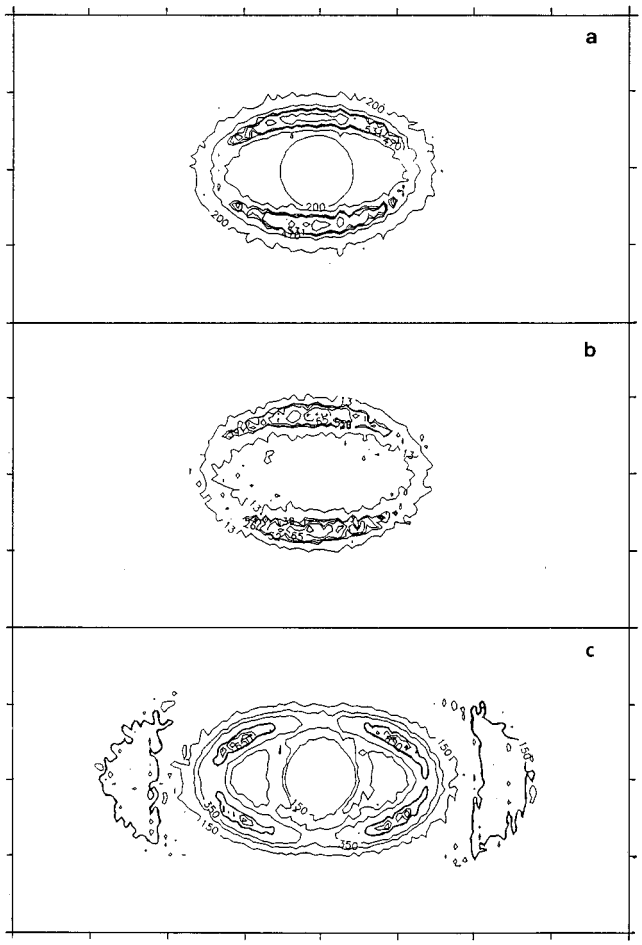

Figure 17. (a) Difffraction from a film stretched at high water content (30% D_2O) and high temperature up to $\lambda = 1.5$. The stripes indicate the repetition of thin objects along the stretching direction. The dip of intensity in the perpendicular direction indicates loss of correlations in this direction. (b) The same sample partly dehydrated (6% D_2O) at $T = T_g - 20$ °C. The loss of correlations has not been recovered. (c) The same sample completely dehydrated and then rehydrated to 15% D_2O. The pattern has returned to that of a sample stretched at this water content, indicating that the loss of correlation suffered during stretching at a higher water content has been recovered.

were performed at a temperature $T = T_g + 25$ °C, where the cores are fairly mobile. In these conditions, the pattern with stripes is obtained only at sufficient stretching, on the order of $\lambda = 3$. If, however, the films are stretched near T_g, the change to a stripe pattern occurs much sooner: for instance, in films stretched when swelled with water (19% of the film weight) and then stretched at $T_g + 2$ °C, the change has already occurred at $\lambda = 1.36$. Therefore, the loss of correlations indicated by the change to a stripe pattern occurs sooner when the membranes are made comparatively weaker than the cell cores.

Finally, we also examined what would happen if the membranes were returned to their strong state after the sample had been stretched. If the stretching was low ($\lambda < 3$), it was found that the structural modifications were reversed by complete dehydration in the stretched state; if it was high, they were not. Figure 17a shows the diffraction pattern of a film stretched at high water content (30% D_2O) and high temperature up to $\lambda = 1.5$. Because of the high water content, correlations in the perpendicular direction are almost completely lost (as in Figure 14). This film was partly dehydrated (to 6%

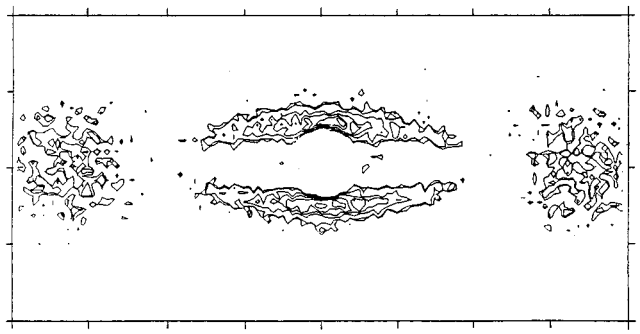

Figure 18. Diffraction from a film swollen with CD_3OD (23% of the film weight) and stretched in the swollen state. The contrast is between the rigid PS cores (32% of the radius) and the soft PBA−PAA matrix. The stripes indicate the repetition of objects at large distances along the stretching direction. The spots correspond to repetition at short distances in the perpendicular direction.

D_2O) at low temperature (T_g − 20 °C) and constant stretching. The diffraction pattern (Figure 17b) shows that the transverse correlations have not been recovered. Subsequently, the film was completely dehydrated and then rehydrated to 15% D_2O, beyond the previous stage. The diffraction pattern (Figure 17c) is similar to that of a sample stretched directly to 15% D_2O (compare with Figure 16); thus, the loss of correlations that occurred at 30% D_2O had been recovered. This recovery of correlations could not be obtained in films that had been stretched beyond $\lambda = 3$, indicating that some irreversible plastic flow takes place at high deformation in the wet state.

(ii) Films with Acid Membranes, Swollen with Methanol. These films were obtained from latex dispersions with acid membranes in water with added salt. They were placed in a closed container saturated with CD_3OD vapor at room temperature. When the swelling was sufficient (23% of the film weight), they were stretched in a few minutes (since methanol lowers the glass transition temperature of the films, there was no need to raise the temperature during stretching). Finally the films were examined through neutron scattering while their deformations and their methanol contents were maintained. A typical diffraction pattern is shown in Figure 18. The first diffraction ring has been reduced to two stripes, as in the case of films swollen with water (compare with Figure 14). However, the intensity of the second ring has been localized in the other, perpendicular direction.

These patterns may be analyzed to give a picture of the objects that cause the scattering. The stripes must be caused by "strings" that are oriented along the stretching, in directions that correspond to the first diffraction line, i.e., either [111] or [200]. The repetition of objects in a string is the repetition of cells in these directions; therefore, each string is made of cells that have a small core inaccessible to methanol and a large outer shell that contains the deuterated methanol. The spots in the perpendicular direction indicate that these strings are regularly spaced in directions perpendicular to the stretching. This correlation is not observed for the films stretched after swelling with water (see above). The crystallographic directions where this correlation is retained are those that contribute most to the second diffraction ring, i.e., [220] (multiplicity 12), [311] (24), [331] (24), and [420] (24) in addition to second-order reflections in directions [111] (multiplicity 8) and [200] (6).

Discussion

In this work we have compared the macroscopic and microscopic deformations of cellular materials submitted to uniaxial stress. The experiments were done according to the following scheme: (a) choose the physical conditions that determine the properties of cell cores and membranes, e.g., temperature or swelling by a preferential solvent; (b) apply uniaxial stress to the sample and maintain the resulting strain; (c) mark one component with deuterated species; and (d) observe the microscopic deformations of the structure through neutron scattering.

In some cases, the microscopic deformations matched the macroscopic stretching; then we have concluded that all cells in the material were stretched in the same way (homogeneous deformation) and that there were no other deformations. In other cases, they did not match; then we have concluded that other deformations (heterogeneous) took place. Both situations are interesting, because the patterns of deformation are characteristic and reproducible. Indeed, the mode of deformation appears to be determined exclusively by the geometry and the relative strengths of the two components of the composite.

"Weak" Dispersed Phase, "Strong" Continuous Phase. This situation was obtained in films that were stretched in the dry state, at high temperature or after swelling by an apolar solvent. These conditions are chosen so that the cores will have a plastic behavior at large deformations. Conversely, the membranes remain elastic because their glass transition temperature is very high and because they are not swollen by apolar solvents.

Mechanical testing shows that the elastic modulus of the films is controlled by the cell cores, while the mechanical failure is determined by the state of the membranes. Indeed, the modulus changes according to the state of the cores: it rises if they are cross-linked, and it drops when they are swollen by an apolar solvent. On the other hand, the films break at a maximal strain, which changes according to the state of the membranes: films with neutralized membranes break at a lower strain than films with acid membranes.

The diffraction patterns correspond to a perfectly affine deformation of the material. Consequently, the cells and the network of membranes must be deformed according to the macroscopic deformation. Moreover, there is no loss of correlation between neighboring cells and therefore no slip or shear within the membranes.

This result is consistent with expectations based on the relative strengths of cores and membranes. The membranes form a network which is elastic, regular, and fully connected. Under uniaxial stress, this network alone would respond with a homogeneous deformation, which would be in every point affine to the macroscopic deformation. Since the cell cores are weaker than the membranes, they do not modify this mode of deformation. Indeed, the only strong constraint set by the cores is that the volume of each cell must remain constant; this constraint is satisfied with an affine deformation field.

In principle, this result could be generalized to any composite material where the dispersed phase is weaker than the continuous phase: we would then expect the deformation field to be controlled by the stronger continuous phase and to be homogeneous throughout the material if the structure was itself regular. However, in many composites, the structure may be too

irregular to produce an affine deformation field in response to a macroscopic strain. Similarly, polymer gels that are swollen by a solvent may not produce affine deformations because the topology of the connections is too irregular.[15] Thus, latex films may be the only type of network that is sufficiently regular to produce a completely affine deformation.

"Strong" Dispersed Phase, "Weak" Continuous Phase. This situation was obtained in films swollen by a polar solvent, water or methanol. In this case, the PS cores remain rigid, while the PBA outer shells and PAA membranes are softened. The films may then be described as dispersions of hard spheres in a viscoelastic matrix.

Mechanical testing of the rehydrated films (water content in excess of 10%) shows that large macroscopic deformations ($\lambda > 3$) are not recoverable; therefore, the mechanical response has changed from elastic to plastic. Mechanical testing of the films swollen with methanol shows plastic behavior at even smaller strains, of the order of $\lambda = 1.1$.

The diffraction patterns do not correspond to an affine (i.e., homogeneous) deformation of the material. Indeed, the distribution of intensity on the diffraction ellipse is opposite to that observed in dry films. This loss of affinity may have two origins: either (a) the deformation within each cell is inhomogeneous, because the weak hydrophilic region is deformed more than the strong hydrophobic core; meanwhile, the lattice is deformed in an affine way; or (b) the lattice is not deformed affinely, and therefore some of the original correlations between cells are lost.

In the following, a calculation of diffraction pattern according to situation (a) is presented, then this is compared with the measured diffraction patterns and the differences are attributed to loss of correlations in the lattice according to situation (b).

Inhomogeneous Deformation of Each Cell. Upon rehydration, the hydrophilic regions become weaker; therefore, they may deform to a larger extent than the dry hydrophobic cores. Let λ_c be the average strain of the cores and λ_r that of the whole cell; λ_r may be taken as equal to the macroscopic strain, since the deformation of the lattice is affine in this case. The ratio λ_c/λ_r is constrained by the condition that the thickness of the hydrophilic region must remain nonzero even in the most stretched regions. Assuming that the average thickness of the hydrophilic region is 15% of the outer particle radius, this yields $\lambda_c/\lambda_r < 1.2$ for the stretched state.

Because of this inhomogeneous deformation, the distribution of water in the cell does not follow the deformation of the lattice. In the parallel direction, the water layer is thicker than expected from an affine deformation of the lattice, and in the perpendicular directions, it is thinner. Consequently, the form factor that describes interferences in the unit cell is modified. This is most apparent at Q values where the form factor vanishes, because the diffraction orders are canceled at those values. In some directions, the extinction will occur at a location that corresponds to the main diffraction lines, while in other directions the extinction may be shifted away from these lines.

The pattern calculated for a deformation at $\lambda_r = 1.5$ is presented in Figure 19a. The intensity of the first diffraction order is located in four spots, instead of the two spots obtained for an affine deformation (Figures 10 and 13). This distribution of intensity matches

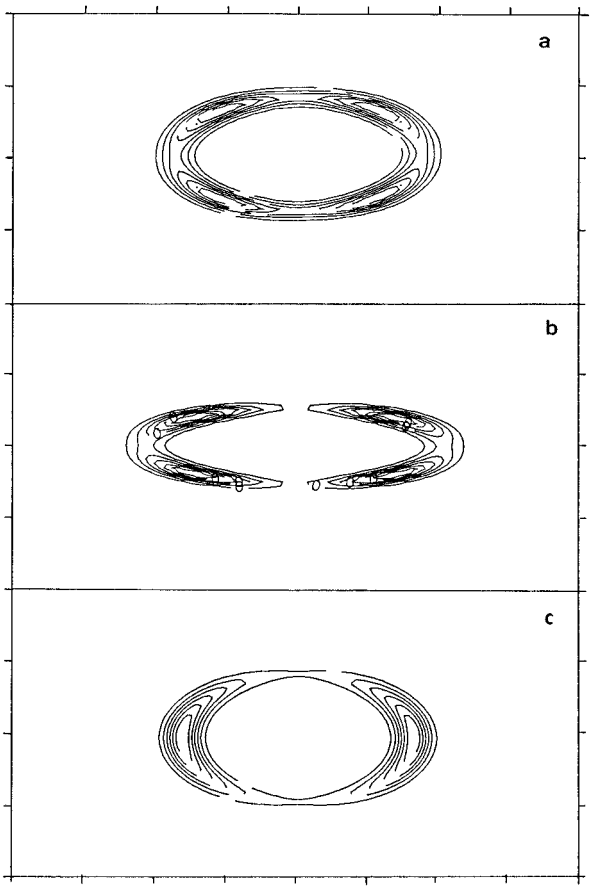

Figure 19. Calculated diffraction patterns for a stretched lattice with inhomogeneous deformation of the unit cell. (a) Swelling by D_2O, stretching to $\lambda = 1.5$. (b) Swelling by D_2O, stretching to $\lambda = 2.5$. (c) Swelling by CD_3OD, stretching to $\lambda = 1.5$.

remarkably the patterns observed for samples stretched at intermediate water contents (Figure 16). However, the agreement ceases at higher stretching or higher swelling: Figure 19b shows that the calculated pattern resembles the two spots of affine deformations, whereas the samples stretched at high water contents give stripes in the opposite direction (Figure 14). The same problem occurs in the case of swelling with methanol, where the calculated pattern for this type of non affine deformation (Figure 19c) is still close to the affine pattern, whereas the experimental patterns again show the two stripes.

Therefore, the deformations that occur with a strong dispersed phase and a weak continuous phase must involve a change of structure in the lattice and not only in the unit cell.

Loss of Correlations in the Lattice. As explained in the Structures of Deformed Films section, the stripe patterns correspond to strings of water pockets; these water pockets are elongated in the stretching direction and repeated at the lattice spacing in this direction. Since there is no diffraction in the perpendicular direction, the strings are irregularly spaced in this direction.

These strings may be characterized according to where they are and how they are oriented. First, they must occur everywhere in the sample. Indeed, the stripes contain most of the intensity in the diffraction pattern. Therefore, they must be produced by objects that contain most of the water. Second, the spacing of these water pockets in a string matches the spacing of cells along a direction where they are nearest neighbors

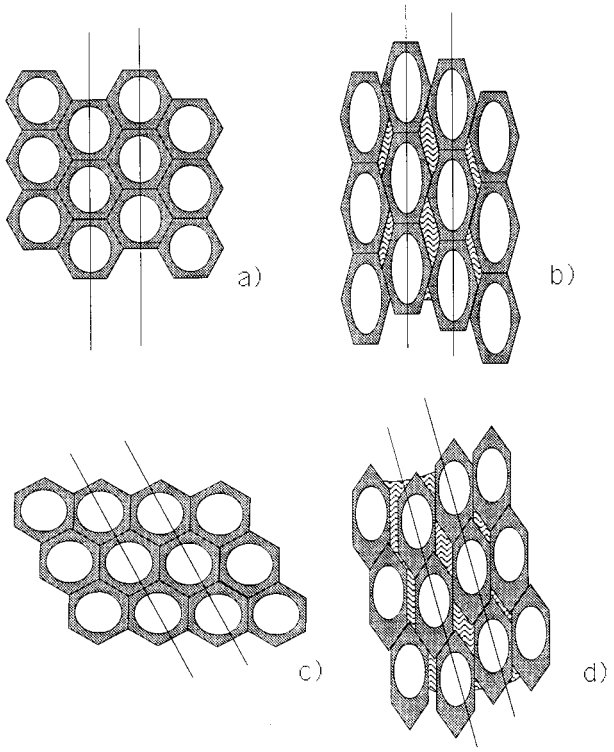

Figure 20. (a) Crystallite of a latex film after swelling by water. The vertical axis of the figure is a dense direction of the lattice. (b) The same crystallite stretched along the vertical axis. In addition to the affine deformation of the cells, the stretching has caused some random shifts between rows of cells aligned along the vertical axis. These shifts are accommodated by water "pockets", which cause the "stripes" in the diffraction patterns of Figure 14. (c) Crystallite of a latex film after swelling by water. In this case, the vertical axis is not a dense direction of the lattice. (d) The same crystallite stretched along the vertical axis. The cells are deformed in the direction of the macroscopic stretching, but the shifts between cells are possible only along a dense direction of the lattice.

(first diffraction order, [111] and [200] directions). Therefore, the structure may also be described as made of columns of cells arranged in a direction where successive cells in a column are nearest neighbors in the lattice (Figure 20). In this sense, the lack of scattering in the perpendicular direction indicates that the correlations between columns are lost. This description implies that the stretching of a wet sample causes irregular shifts between columns of cells.

This description makes sense from a mechanical point of view. Indeed, the directions where correlations are retained are among the more dense directions of the material (cells are nearest neighbors along those directions), while the directions where correlations are lost are the less dense directions in the material. As shown in Figure 20, a shift of columns along the dense directions is much easier than a shift along other directions. Thus, the random shifts observed between columns of cells imply that the material is unstable in shear along certain directions. This instability occurs when the hydrophilic membranes have been swelled by water; the amount of water (15% of the film weight) corresponds to swelling by a factor of 3 or 4. Therefore, there is a critical swelling beyond which the membranes become too weak compared with the cell cores to maintain the stability of the material.

Plastic Behavior upon Swelling with Methanol. Films that have been swollen with methanol have some features that are common with rehydrated films and others that are significantly different. The differences can be attributed to the extensive penetration of methanol into the cells. Indeed, the only regions that exclude methanol are the central PS cores, with radii equal to 34% of the outer cell radius. The outer regions of the cells, which are swollen by methanol, hold 86% of the film volume.

Mechanical testing of these films shows that most deformations are not recoverable. Indeed, plastic behavior sets in at much lower strains ($\lambda = 1.1$) than in the case of rehydrated films ($\lambda = 6$). This plastic behavior resembles that of soft, non-cross-linked polymers.

The diffraction patterns show that the microscopic deformations are not affine to the macroscopic deformations. As in the case of rehydrated films, the first-order intensity is concentrated in a set of two stripes that are centered on the stretching direction and elongated in the perpendicular direction. Again, there are two possible causes for such a nonaffine distribution of scattered intensity: a nonhomogeneous deformation of each cell, or a change in correlations between cells. In the present case, the nonhomogeneous deformation of each cell results from the fact that the PS cores are undeformed. Since the volume of the PS cores is only 3% of the film volume, this nonhomogeneous deformation must have a negligible effect on the diffraction spectrum. Therefore, the nonaffine distribution of intensity must be produced by a change in the correlations between cells.

The diffraction patterns also show that this change of correlations is not the same as that for rehydrated films. Indeed, these patterns show a strong intensity in the perpendicular direction, at the location of the second diffraction order. This diffraction is absent in the rehydrated films. A crystallographic description of the deformations, such as was proposed for rehydrated films, is rather awkward. The argument would have to go as follows.

The stripes located in the stretching direction indicate that correlations are retained along crystallographic directions that are oriented along this direction. Since this localization corresponds to the first-order ring, these directions must be [111] or [200] directions. Thus, correlations would be retained along [111] directions that are oriented along the stretching but lost along [111] directions that are perpendicular to the stretching. The spots located in the perpendicular direction indicate that correlations are retained along other crystallographic directions. Since this localization corresponds to the second-order ring, these directions must be [220], [311], [331], or [420] directions. Thus, correlations are retained along such directions that are perpendicular the stretching but lost along similar directions that are parallel to the stretching. A picture for deformations of this type is proposed in Figure 21.

It is a bit unlikely that a material made of a soft, viscoelastic matrix (96% of the volume) containing small rigid cores (4% of the volume) can have such a specific response to a stretching deformation. An alternative interpretation would be to ignore the crystallographic directions and consider the displacements of small spheres embedded in a matrix that is forced to flow. In an elongational flow, the matrix is compressed in the perpendicular direction, and therefore some of these rigid spheres will be pushed in contact with each other. They will form doublets or triplets oriented mainly along the perpendicular direction. Conversely, the matrix is

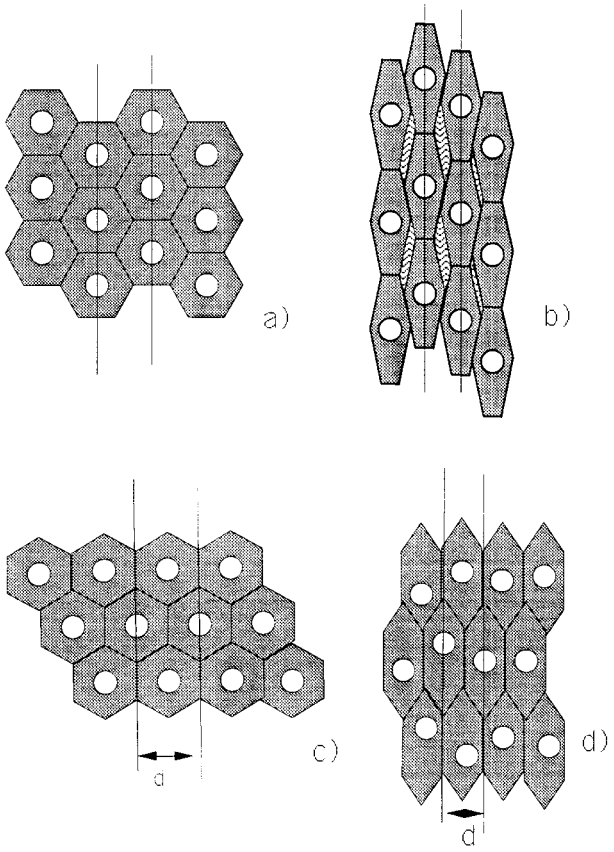

Figure 21. (a) Crystallite of a latex film after swelling by methanol. The vertical axis of the figure is a dense direction of the lattice. (b) The same crystallite stretched along the vertical axis. The stretching has caused random shifts between rows of cells aligned along the vertical axis. These shifts may be the cause of the stripes observed in Figure 18. (c) Crystallite of a latex film after swelling by methanol. In this case, the vertical axis is not a dense direction of the lattice. The spacing d is the distance between lattice planes that are oriented along the vertical direction; diffraction by these planes gives the intensity observed in the second diffraction order. (d) The same crystallite stretched along the vertical axis. The cells are deformed in the direction of the macroscopic stretching. Random shifts between columns of cells are also possible in this direction, because the continuous phase has been softened by the methanol.

elongated along the stretching direction, and therefore some matrix material will flow between these multiplets in order to cope with this elongation. This will cause increased separation between multiplets along the stretching direction. The resulting structure will be made of small multiplets that are oriented along the perpendicular direction and regularly spaced along the stretching direction. This structure would reproduce the observed diffraction patterns: interferences between spheres within a multiplet would give two diffraction spots at large Q in the perpendicular direction; interferences between multiplets would give stripes in the stretching direction.

Comparison of Deformations after Swelling with Water or with Methanol. The differences between the correlations observed in presence of water and in presence of methanol must originate from the different localizations of water and methanol.

In films rehydrated with water, the PAA membranes are swelled considerably (by a factor of 3 or 4), and they are much weaker than the dispersed phase; therefore, the deformation tends to localize preferentially within them. Because these membranes are thin (about 10% of the particle radius), their deformations may be quite large, even if the overall strain is moderate. The first response to a macroscopic stretching is a nonaffine deformation of each cell, by which water and membrane polymers are pushed out of regions that are compressed and into regions that are expanded. This deformation is limited by the anchoring of membrane polymers. Consequently, at high deformations and for large swelling ratios, additional deformations take over. These deformations reduce the local stress by shifting columns of cells in such a way that the cell cores of neighboring columns avoid each other. Because the membranes are thin, these shear deformations are possible only along dense directions of the lattice; in these directions, the resistance against shear is low because the shear deformation is facilitated by flow of water from compressed regions into expanded ones. Because the swelling of the thin membranes is irregular, the distances between these columns are also irregular. The resulting behavior is that of a hard material with a few weak planes of shear.

In films swollen with methanol, the PAA membranes and the PBA−PS outer shells of the particles are both weakened by the solvent. Therefore, elongational deformations are distributed throughout the PBA−PAA matrix, which occupies most of the volume, and they are possible in all directions of the lattice.The nonaffine diffraction patterns reflect the motions of the rigid PS cores embedded in this matrix. These motions are nonaffine because the PS cores cannot overlap. Thus, the observed behavior is that of a soft polymer that is decorated by rigid, repelling spheres.

Conclusion

Latex films are composite materials with a cellular structure. The cell cores are the dispersed phase of the composite, while the membranes form the continuous phase. Through selective swelling of either phase, the material can become soft in the dispersed phase or soft in the continuous phase.

The response of these materials to a macroscopic stretching depends on which phase is the weaker phase of the composite. Indeed, in a macroscopic stretching, the dispersed phase tends to respond with a stretching of each cell, whereas the continuous phase tends to respond with a slip between cells.

In the situation where the cell cores are the strong component, we have demonstrated that the microscopic response to a macroscopic stretching is, indeed, a homogeneous stretching of all cells. Conversely, in the situation where the membranes are the weak component, the deformations are localized in the membranes, the cells slip past each other, and the lattice is disorganized by these microscopic shear deformations.

Appendix A

The localization of deuterated solvents in the unit cell was determined from the comparison of experimental scattering curves with the calculated scattering for unit cells of different structures. In this calculation, it was necessary to use a unit cell with a dodecahedral outer shape, since this shape is imposed by the packing of the cells. Moreover, it was found that the central core excluding water is also a dodecahedron. Indeed, calculations with a spherical central core and a dodecahedral outer boundary do not fit the scattering of films swelled by water, obviously because the thickness of the water membranes is not constant in this case.

This appendix presents the expressions for the form factors $P_i(q_i)$ calculated at each of the diffraction orders q_i in a lattice made of a dodecahedral cells. Each cell has a distance between opposing faces a; water penetrates an outer shell of constant thickness b but is excluded from a central dodecahedral core:

$$P_{111}(q) = \{[(24\sqrt{3})/q^3][2\sin[q(a-b)\sqrt{2/3}] - \sin[q(a-b)\sqrt{3/2}] - \sin[q(a-b)\sqrt{1/6}]]\}^2 \quad (2)$$

$$P_{110}(q) = \{[(2\sqrt{2})/q^2][2(a-b) + ((a-b)^2 q \sin[q(a-b)] - 2(a-b)\cos[q(a-b)])]\}^2 \quad (3)$$

$$P_{200}(q) = \{[16/q^3](2\sin[q(a-b)\sqrt{1/2}] - \sin[q(a-b)\sqrt{2}])\}^2 \quad (4)$$

$$P_{311}(q) = \{[(88\sqrt{11})/(45q^3)](-4\sin[q(a-b)\sqrt{1/11}] - 6\sin[q(a-b)3\sqrt{2/11}] + \sin[q(a-b)\sqrt{1/22}] + 6\sin[q(a-b)3\sqrt{1/22}] + 5\sin[q(a-b)5\sqrt{1/22}])\}^2 \quad (5)$$

$$P_{331}(q) = \{[(152\sqrt{19})/(5\sqrt{49}q^3)] \times (2\sin[q(a-b)\sqrt{1/19}] + 12\sin[q(a-b)3\sqrt{2/19}] - 2\sin[q(a-b)\sqrt{1/38}] - 5\sin[q(a-b)5\sqrt{1/38}] - 7\sin[q(a-b)7\sqrt{1/38}])\}^2 \quad (6)$$

For the film swollen with D_2O, the fit shown in Figure 6a was obtained through eq 1 with a dodecahedral cell of parameter $b/a = 0.13$, using $\sigma_1 = 9.6 \times 10^{-4}$ Å^{-1}, $\sigma_2 = 1.17 \times 10^{-3}$ Å^{-1}, and $\sigma_3 = \sigma_4 = \sigma_5 = \sigma_6 = 2 \times 10^{-3}$ Å^{-1} for the widths of the Gaussian lines that describe the successive diffraction orders. The low value of b/a and the shape of the cell, which must be a dodecahedron, confirm that D_2O is confined in the thin cell membranes.

For the film swollen with methanol, the fit (Figure 7b) was obtained with cells of parameter $b/a = 0.8$; the precise shape of the cell is indifferent because the form factors of spherical shells and dodecahedral shells become indistinguishable when b/a is close to unity. The other parameters of the fit are $\sigma_1 = 9.6 \times 10^{-4}$ Å^{-1}, $\sigma_2 = 1.17 \times 10^{-3}$ Å^{-1}, and $\sigma_3 = \sigma_4 = \sigma_5 = \sigma_6 = 3.33 \times 10^{-3}$ Å^{-1}. The large value of b/a confirms that methanol is excluded only from a small central core made of pure PS.

Appendix B

This appendix presents the calculation of the azimuthal variation of the diffracted intensity caused by an affine deformation of the film. It is assumed that the films are polycrystalline and that the crystallites have random orientations in the undeformed film. Therefore, the orientational density of crystallites per solid angle is uniform and equals $1/4\pi$. The resulting Lorentz factor, which corrects the intensity for the number of crystallites in the Bragg condition, is isotropic and decays as $1/q^2$. An affine deformation of this polycrystal causes each cell to be elongated by a factor λ in the parallel direction and to be shrunk by a factor $\lambda^{-1/2}$ in the perpendicular direction. In the following, we calculate an anisotropic Lorentz factor for each diffraction peak.

Consider the scattering by a single crystallite in a direction defined by a scattering vector **q**. Let θ be the azimuthal angle between **q** and the stretching direction. A deformation of this crystallite will shift this scattering into a direction **q′** located at an angle θ' from the stretching direction. If the local deformation is affine to the uniaxial stretching of the sample, then the relation between θ and θ' will be

$$\tan\theta' = \lambda^{3/2}\tan\theta$$

For a polycrystalline sample, the set of all vectors **q** that were, before deformation, located within a solid angle $d\Omega$ becomes shifted into a new solid angle $d\Omega'$. Similarly, the intensity located in $d\Omega$ becomes shifted in $d\Omega'$; its value may be calculated as

$$I(\theta')/I_{iso} = d\Omega'/d\Omega = \lambda^{3/2}/(\lambda^3\cos^2\theta' + \sin^2\theta')^{3/2}$$

This redistribution of the intensity causes a decrease by a factor λ^3 in the parallel direction and an increase by a factor $\lambda^{3/2}$ in the perpendicular direction. This result can be understood as follows: (i) the part of the diffraction sphere that is in the stretching direction has been squeezed by $1/\lambda$ in this direction and stretched by $\lambda^{1/2}$ in each of the perpendicular directions, which gives a λ^3 decrease of the intensity, and (ii) the part of the diffraction sphere that is in the perpendicular direction has been stretched by $\lambda^{1/2}$ in both perpendicular directions and squeezed by $1/\lambda$ in the parallel direction, which gives a $\lambda^{3/2}$ decrease of the intensity.

The scattering pattern calculated in this way for the 111 diffraction line of a polycrystalline sample has been shown in Figure 13b.

References and Notes

(1) Dobler, F.; Pith, T.; Lambla, M.; Holl, Y. *J. Colloid Interface Sci.* **1992**, *152*, 1.
(2) Winnik, M. A.; Wang, Y. *J. Coatings Technol.* **1992**, *64*, 51.
(3) Distler, D.; Kanig, G. *Colloid Polym. Sci.* **1978**, *256*, 1052.
(4) Zozel, A.; Heckmann, W.; Ley, G.; Mächtle, W. *Makromol. Chem., Macromol. Symp.* **1990**, *35−36*, 423.
(5) Joanicot, M.; Wong, K.; Maquet, J.; Chevalier, Y.; Pichot, C.; Graillat, C.; Lindner, P.; Rios, L.; Cabane, B. *Prog. Colloid Polym. Sci.* **1990**, *81*, 175.
(6) Chevalier, Y.; Pichot, C.; Graillat, C.; Joanicot, M.; Wong, K.; Maquet, J.; Lindner, P.; Cabane, B. *Colloid Polym. Sci.* **1992**, *270*, 806.
(7) Wang, Y.; Kats, A.; Juhué, D.; Winnik, M. A. *Langmuir* **1992**, *8*, 1435.
(8) Rieger, J.; Hädicke, E.; Ley, G.; Lindner, P. *Phys. Rev. Lett.* **1992**, *68*, 2782.
(9) Pieranski, P. *Contemp. Phys.* **1983**, *24*, 25.
(10) Monovoukas, Y.; Gast, A. *J. Colloid Interface Sci.* **1989**, *128*, 533.
(11) Winnik, M. A.; Wang, Y. *J. Coatings Technol.* **1992**, *64*, 51.
(12) Guinier, A. *Théorie et technique de la radiocritallographie*; Dunod: Paris, 1964.
(13) Doi, M.; Edwards, S. F. *Properties of polymers*; J. Wiley: New York, 1982.
(14) Wong, K.; Joanicot, M.; Richard, J.; Maquet, J.; Cabane B. *Macromolecules* **1993**, *26*, 3168.
(15) Mendes, E.; Lindner, P.; Buzier, M.; Boué, F.; Bastide, J. *Phys. Rev. Lett.* **1991**, *66*, 1595.

MA951142U